Robotics and Autonomous Systems 61 (2013) 1306–1313

Contents lists available at ScienceDirect

Robotics and Autonomous Systems

journal homepage: www.elsevier.com/locate/robot

A geometric approach for inverse kinematics of a 4-link redundant *In-Vivo* robot for biopsy

L. Sardana, M.K. Sutar, P.M. Pathak *

Robotics and Control Laboratory, Mechanical and Industrial Engineering Department, Indian Institute of Technology, Roorkee, 247667, India

HIGHLIGHTS

- A geometric approach for inverse kinematic solutions of redundant manipulators.
- A model for a 4-link redundant manipulator of an In-Vivo biopsy robot was developed.
- Simulations were carried out in MATLAB using the developed approach.
- Experiments were conducted on a 4 scaled model of the In-Vivo robot.
- Simulation results were validated against the experimental results.

ARTICLE INFO

Article history:
Received 7 March 2013
Received in revised form
18 August 2013
Accepted 2 September 2013
Available online 18 September 2013

Keywords:
Inverse kinematics
Redundant manipulators
In-Vivo robot
Geometrical method

ABSTRACT

The presence of a large number of degrees of freedom enables redundant manipulators to have some desirable features like reaching difficult areas and avoiding obstacles. These manipulators in the form of *In-Vivo* robots will enhance the dexterity and capacity of a surgeon to explore the internal cavity when inserted in the existing tool channel of the endoscope to take a biopsy from the stomach. This paper presents a simple geometric approach, to solve the problem of multiple inverse kinematic solutions of redundant manipulators, to find a single optimum solution and to easily switch from one solution to another depending upon the path and the environment. A simulation model of this approach has been developed and experiments have been conducted on the *In-Vivo* robot to judge its effectiveness.

1. Introduction

Continuous manipulators are generally preferred over conventional manipulators in the case of surgery robots due to their high dexterity and manoeuvrability [1]. But the continuous manipulators are difficult to control because they have a very large number, even infinite degrees of freedom (DOF). To simplify the control and get some closer behaviour of continuous manipulators, redundant manipulators are considered. These are termed as redundant manipulators due to their higher number of actuable DOF than the DOF of their intended workspace [2]. Conkur and Buckingham suggested the definition of a redundant manipulator as 'any robotic system in which the way of achieving a given task is not unique may be called redundant' [3]. According to McKerrow [4], 'when a manipulator can reach a specified position with more than one configuration of the linkages, the manipulator is said to be redundant'.

Many algorithms for the inverse kinematics of redundant manipulators have been proposed including neural networks [5], genetic algorithms [6,7], algebraic [8] and geometric methods [9]. Mao and Hsia [10] developed an approach to solve the inverse kinematics problem of redundant manipulators in an environment with obstacles using forward kinematics functions and trained the neural network in the inverse modelling manner. Ellipsoids are one of the analytical tools available to access the capabilities of redundant manipulators. Different types of ellipsoids have been formulated and examined to analyse the kinematic model of redundant manipulators [11]. A technique, which is a combination of a closed loop pseudoinverse method with a genetic algorithm, has been proposed by Marcos and Machado [12], which can be used for repeatable control of redundant manipulators for avoiding the joint angle drift problem. Simulation results show when the end-effector traces a closed path the robot returns to its initial posture. The inverse kinematics problem of a 7-DOF redundant manipulator has been resolved using a closed-loop inverse kinematics (CLICK) algorithm [13]. The algorithm has been

* Corresponding author. Tel.: +91 1332285608.
E-mail addresses: lokesume@iitr.ernet.in (L. Sardana), mihirkumarsutar@yahoo.in (M.K. Sutar), pushppathak@gmail.com, pushpfme@iitr.ernet.in (P.M. Pathak).

0921-8890/$ – see front matter © 2013 Elsevier B.V. All rights reserved.
http://dx.doi.org/10.1016/j.robot.2013.09.001

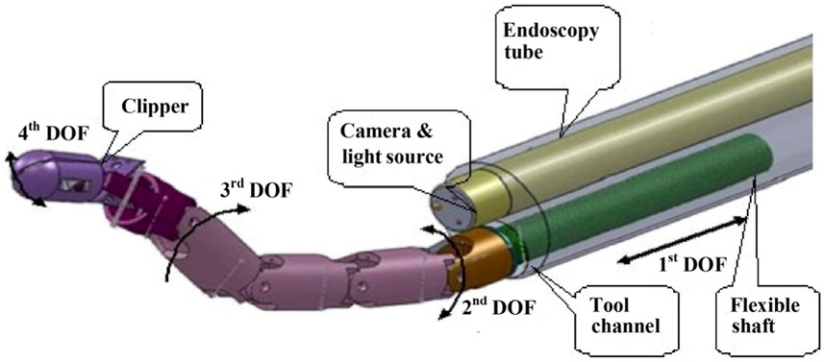

Fig. 1. CAD model of the In-Vivo robot with its DOFs and parts [22].

extended to find redundancy resolutions at the velocity and acceleration level.

Often, adjectives like 'highly' or 'hyper', are frequently used with redundant manipulators in conjunction with terms like snake robots. Such robots have a joint space dimension which is much greater than the dimension of the end-effector space, as mentioned by Burdick et al. [14] and Chirikjian and Burdick [15]. Many researchers have given their contribution kinematic analysis of hyper-redundant manipulator.

A new geometrical method for solving the inverse kinematics of continuum robot manipulators has been suggested by Neppali et al. [16]. The approach first concentrates on a single section of the multi-section trunk shape continuum manipulator then the complete solution for the same has been achieved. A detailed analysis with a kinematic model of a continuum style manipulator with its design, construction and implementation has been presented by Hannan and Walker [1].

An algorithm for solving the inverse kinematic problem of a discretely actuated hyper-redundant manipulator has been proposed by Uphoff and Chirikjian [17]. Chirikjian's contribution to solve the inverse kinematics problem of a hyper-redundant robot is quite palpable [18,19]. An approach for real time shape control of a continuum robot, with coordination of inputs such as tendon lengths and pneumatic pressure with the Cartesian coordinates, has been suggested by Jones and Walker [20]. In this approach the inverse kinematics to relate the manipulator curvature with the cable lengths has also been analysed.

An algorithm for solution of the inverse kinematics problem and to resolve the redundancy issue of hyper-redundant manipulators has been proposed by Sreenivasan et al. [21]. The simulation results of the tractrix based algorithm indicate convincing results.

In this paper, a simple geometric approach has been developed for solving the inverse kinematics of a 4-link redundant manipulator of an *In-Vivo* robot for biopsy [22] in a three dimensional work space. The described approach is simple in nature for solving inverse kinematics of a surgical robot for biopsy. Experimental results have been shown using a 4 scaled *In-Vivo* robot.

2. Developed *In-Vivo* manipulator

The CAD model of the *In-Vivo* robot manipulator with different parts is as shown in Fig. 1 [22]. The robot's 1st DOF provides the linear motion to move the whole robot forward, the 2nd DOF gives the rotary actuation, the 3rd DOF provides the planar motion and the 4th DOF indicates the clipper motion for taking the biopsy.

The 4-scaled model was fabricated using both conventional and advanced manufacturing processes like wire cut EDM and is shown in Fig. 2. The fabricated robot has to be inserted through the tool channel of the endoscopy tube with the camera and light source. The central control architecture is stationed outside and movement of the robot along with the positioning of the camera is controlled with it.

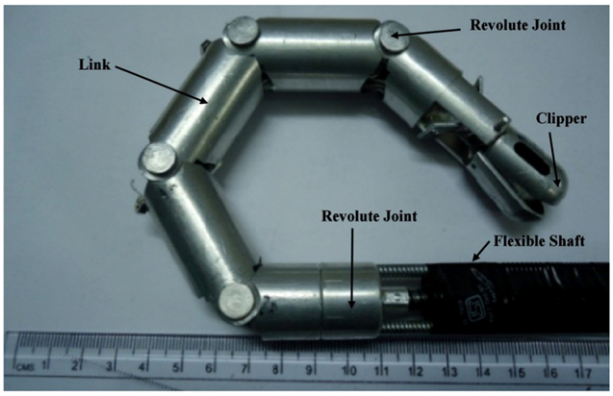

Fig. 2. Fabricated four scaled model of the *In-Vivo* robot [22].

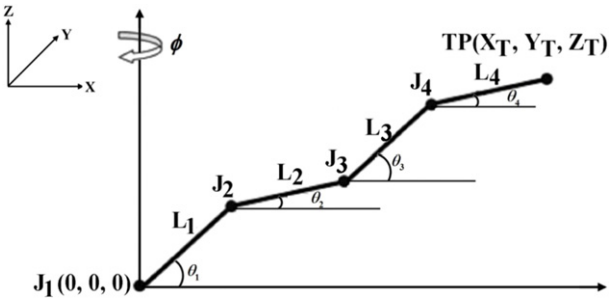

Fig. 3. A 4-link redundant manipulator.

3. The proposed inverse kinematics algorithm

3.1. Geometrical approach

Consider a four link manipulator with 3 DOF as shown in Fig. 3. Here the translational degree of freedom shown in Fig. 1 is not considered for analysis purposes. Since the number of links in the X–Z plane is more than the number of degrees of freedom in that plane, so it is a redundant manipulator. Here, J_i denotes the ith joint, θ_i denotes the joint angle of the ith joint, L_i denotes length of the ith link and ϕ denotes the twist of the first joint (J_1).

Let the first joint J_1 be located at the origin and TP (X_T, Y_T, Z_T) be the target point of the manipulator's tip to be achieved. The target point TP is chosen in such a way that the distance of the TP from J_1 is less than or equal to the sum of lengths of all links.

$$L_{J_1\text{-TP}} \leq L_1 + L_2 + L_3 + L_4. \tag{1}$$

The proposed method can be explained in the following steps:

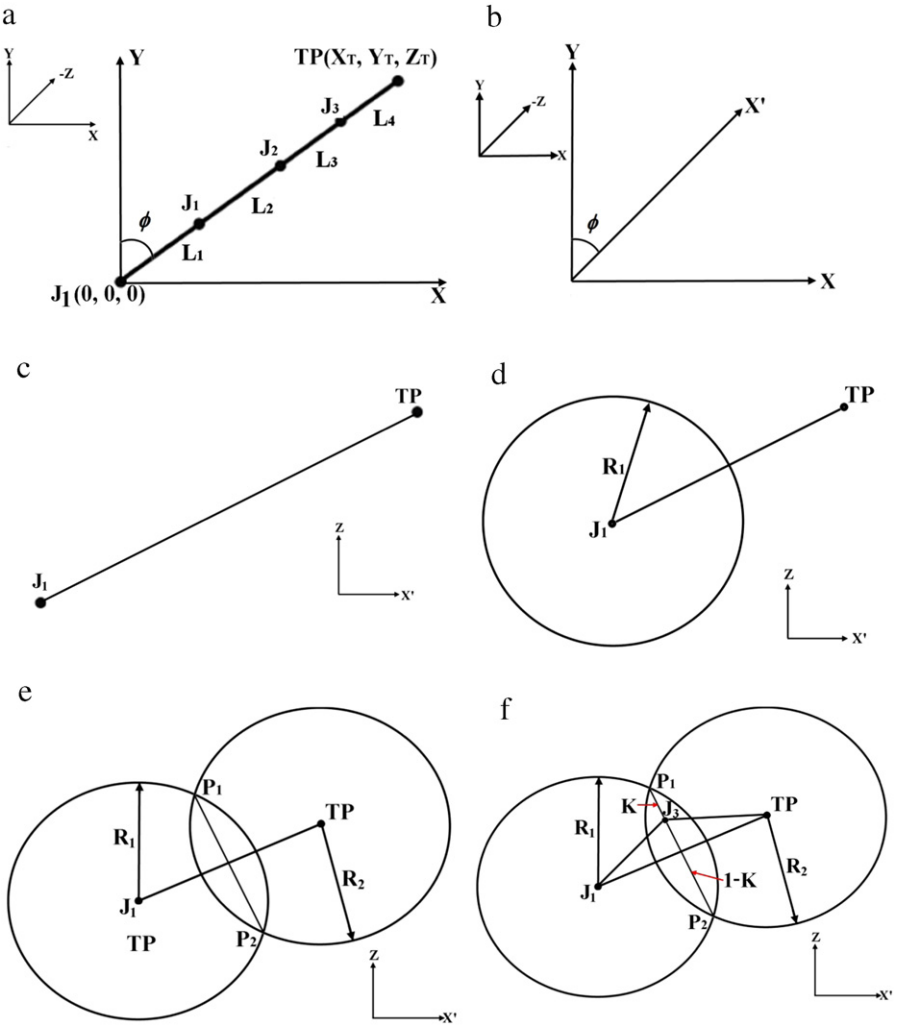

Fig. 4. (a) Step 1, (b) step 2, (c) step 3, (d) step 4, (e) step 5, (f) step 6.

1. Calculate the desired twist ϕ by measuring the angle between the final position of the plane of the manipulator and the Y-axis as shown in Fig. 4(a). The angle ϕ will be given by:

$$\phi = \tan^{-1}\left(\frac{X_T}{Y_T}\right) \tag{2}$$

where X_T and Y_T are the X and Y coordinates of the target point.

2. Draw a new plane X'–Z such that it makes an angle ϕ with the Y-axis as shown in Fig. 4(b), thus the coordinates in this plane are given by

$$X' = \frac{X}{\sin\phi}, \qquad Z' = Z. \tag{3}$$

3. In the plane X'–Z, draw a line joining the origin (J_1) and the Target point (TP) as shown in Fig. 4(c).
4. Draw a circle of radius $R_1 = L_1 + L_2$ with its centre at point J_1 as shown in Fig. 4(d).
5. Draw another circle with its radius $R_2 = L_2 + L_3$ and centre at point TP. This circle will intersect the previous circle (drawn in step 4) at points P_1 and P_2 respectively. Draw a line P_1P_2 joining points P_1 and P_2 as shown in Fig. 4(e).
6. Locate a point J_3 on line P_1P_2 such that it divides the line P_1P_2 in $K : (1 - K)$, where $0 < K < 1$. The method for deciding the value of K is discussed later in Section 3.2. Draw two lines joining J_1 to J_3 and J_3 to TP respectively as shown in Fig. 4(f).
7. Draw a line J_1J_2 of length L_1 and making an angle μ_1 with the line J_1J_3 as shown in Fig. 5. The line J_1J_2 represents the link 1 of

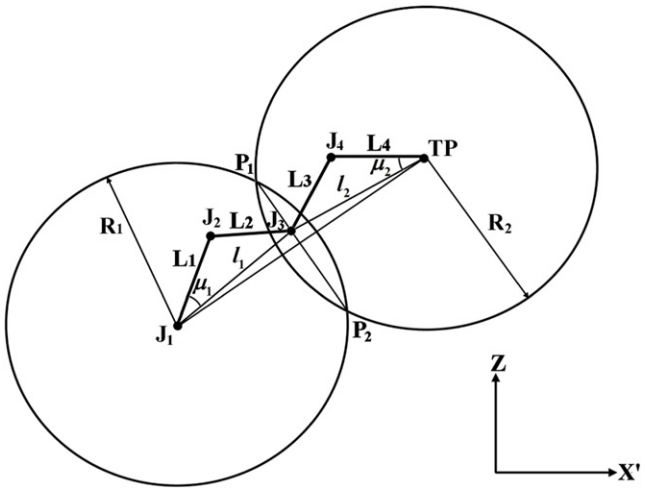

Fig. 5. Final description.

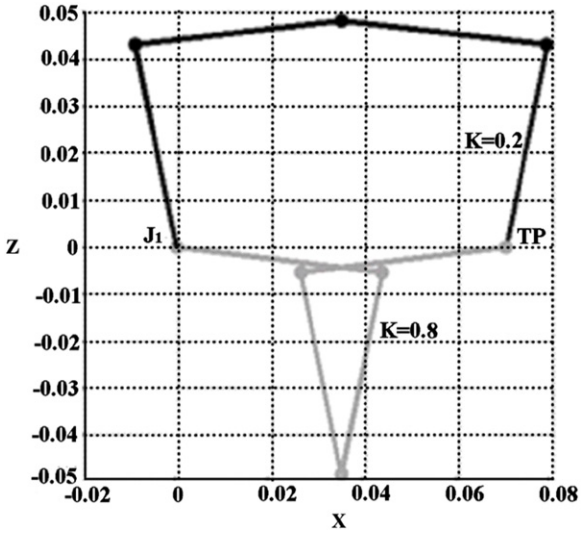

Fig. 6. Effect of K on entanglement, TP (0.07, 0, 0).

the manipulator. Join the points J_2 and J_3 to obtain the line J_2J_3. This line J_2J_3 represents the link 2. The angle μ_1 can be evaluated as

$$\mu_1 = \sin^{-1}\left(\frac{L_2 \sin\varepsilon_1}{l_1}\right) \tag{4}$$

where $\varepsilon_1 = \cos^{-1}\left(\frac{L_1^2 + L_2^2 - l_1^2}{2L_1L_2}\right)$ and l_1 is the length of the line J_1J_3.

8. Similarly, draw another line TP J_4 of length L_4 and making an angle μ_2 with the line TP J_3 as shown in Fig. 5. The line J_4 TP represents the link 4 of the manipulator. Join points J_3 and J_4 to obtain the line J_3J_4. This line J_3J_4 will represent the link 3. Then the angle μ_2 can be expressed as

$$\mu_2 = \sin^{-1}\left(\frac{L_3 \sin\varepsilon_2}{l_2}\right),$$

$$\text{where } \varepsilon_2 = \cos^{-1}\left(\frac{L_3^2 + L_4^2 - l_2^2}{2L_3L_4}\right) \tag{5}$$

where l_2 is the length of the line TP J_3.

9. Calculate the joint angles θ_1, θ_2, θ_3 and θ_4 from the slopes of link 1 (J_1J_2), link 2 (J_2J_3), link 3 (J_3J_4), and link 4 (J_4 TP) respectively.

3.2. Value of parameter K

The inverse kinematics of a redundant manipulator will always give a large number of feasible solutions. The selection of one optimum solution out of a set of a number of feasible solutions will depend on the value of parameter K. The value of K is chosen in such a way that (i) the resultant configuration has a smooth and tangle free configuration and (ii) irregularities can be easily adjusted.

3.2.1. Smooth and tangle free configuration

Some configurations of the manipulator (with the target point TP closer to the origin J_1) may result in the formation of tangles and knots in the manipulator's body. One such case is shown in Fig. 6. For values of $K > 0.5$, a tangle or loop starts forming from the manipulator's body which may create difficulty in manoeuvring and control of the robot inside the stomach.

Also, there are some configurations (with the target point TP at some distance from the origin J_1) which may result in the formation

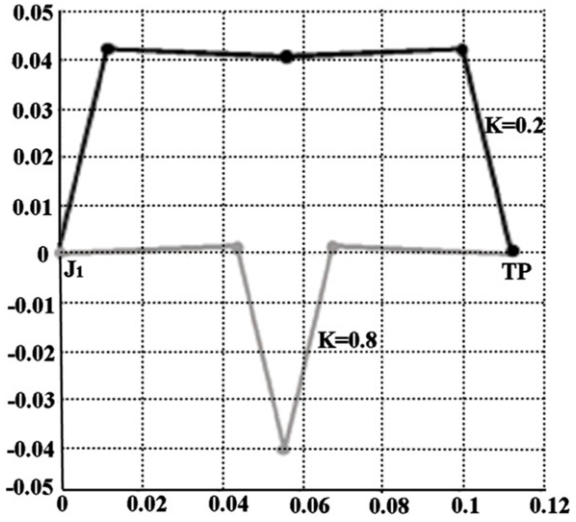

Fig. 7. Effect of K on smoothness, TP (0.115, 0, 0).

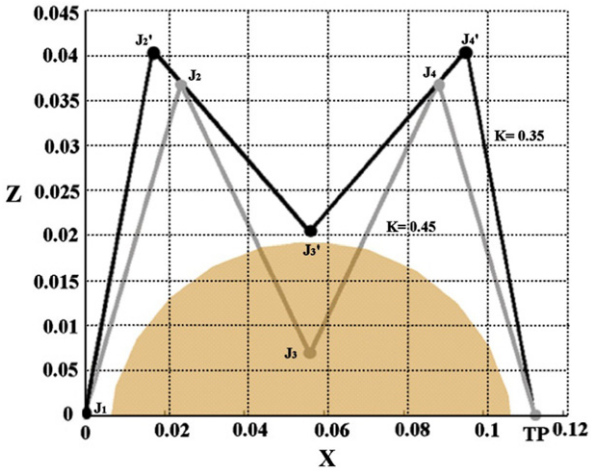

Fig. 8. Adjustment to irregularities.

of a sharp projection or a bend in the manipulator's body. One such case is shown in Fig. 7. For values of $K > 0.5$, there is a sharp bend between link 2 and link 3. These configurations will not be good in the case of an *In-Vivo* robot as such a bend can cause unnecessary damage to the tissues inside the stomach.

Considering these factors, the value of parameter K is chosen in such a way that

$$K = \begin{cases} 0 < K < 0.5 & \forall\{X, Z \in R\} - \{X = 0,\ Z > 0\}, \\ & Y > 0 \text{ (a)} \\ 0.5 < K < 1 & \forall X = 0, Z > 0,\ Y > 0 \\ 0 < K < 0.5 & \forall\{X \in R,\ Z < 0\} \cup \{X > 0,\ Z = 0\}, \\ & Y = 0 \text{ (b)} \\ 0.5 < K < 1 & \forall\{X \in R,\ Z > 0\} \cup \{X < 0,\ Z = 0\}, \\ & Y = 0 \\ 0 < K < 0.5 & \forall X \in R,\ Z < 0,\ Y < 0 \text{ (c)} \\ 0.5 < K < 1 & \forall X \in R,\ Z \geq 0,\ Y < 0. \end{cases} \tag{6}$$

To illustrate the use of Eq. (6), consider the Target Point TP (−0.12, 0.04, 0.03). In this case, Y is positive. So, go to Eq. (6)(a). Now, look for values of X and Z. Here, X and Z are real numbers and the value of X is not zero. So, the value of K is chosen in such a way that it lies between 0 and 0.5.

3.2.2. Adjustment to irregularities

There may be some irregularities on the internal walls of the stomach. Some configurations of the manipulator are not feasible

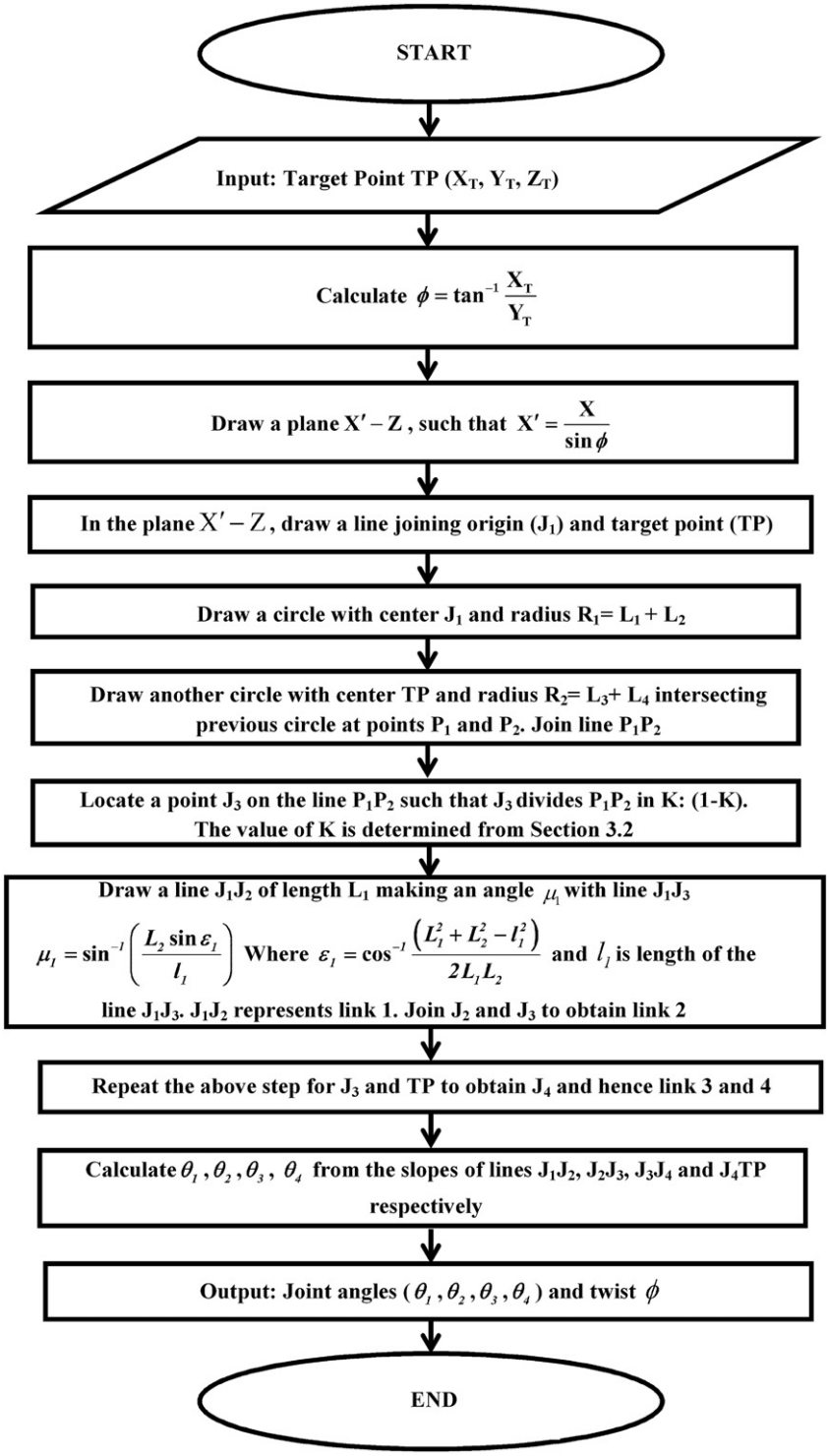

Fig. 9. The flowchart of the proposed method.

due to the presence of these irregularities. So, the manipulator needs to readjust its configuration in order to prevent any part of the manipulator colliding with these irregularities.

Consider the case shown in Fig. 8. In order to readjust the configuration according to the irregularities, the value of K for this case is readjusted such that

$$K < \frac{1}{2} - \frac{h}{P_1P_2} \tag{7}$$

where h is the approximate height of the irregularity and P_1P_2 is the length of the line joining points P_1 and P_2, the intersecting points of two circles (shown in Fig. 5). Fig. 8 illustrates a configuration of the manipulator with the value of K equal to 0.45. The joint positions of this configuration are: J_1, J_2, J_3 and J_4. The approximate height of the irregularity is 0.0185 m. In order to prevent the collision of joint J_3 with the irregularity, the value of K is readjusted to 0.35. Thus new joint positions are: J_1', J_2', J_3' and J_4' preventing any collision

Table 1
Different input target points and output joint variables.

Sl. no.	Input				Output (°)				
	X (m)	Y (m)	Z (m)	K	θ_1	θ_2	θ_3	θ_4	ϕ
1	0.030	0.060	0.040	0.8	127.07	35.47	26.14	−65.46	26.57
2	0.000	0.160	0.000	0.2	34.84	−4.09	4.09	−34.84	0
3	0.000	0.100	0.060	0.8	101.92	28.30	33.63	−39.99	0
4	−0.12	0.04	0.03	0.2	74.68	9.41	17.27	48	−71.57

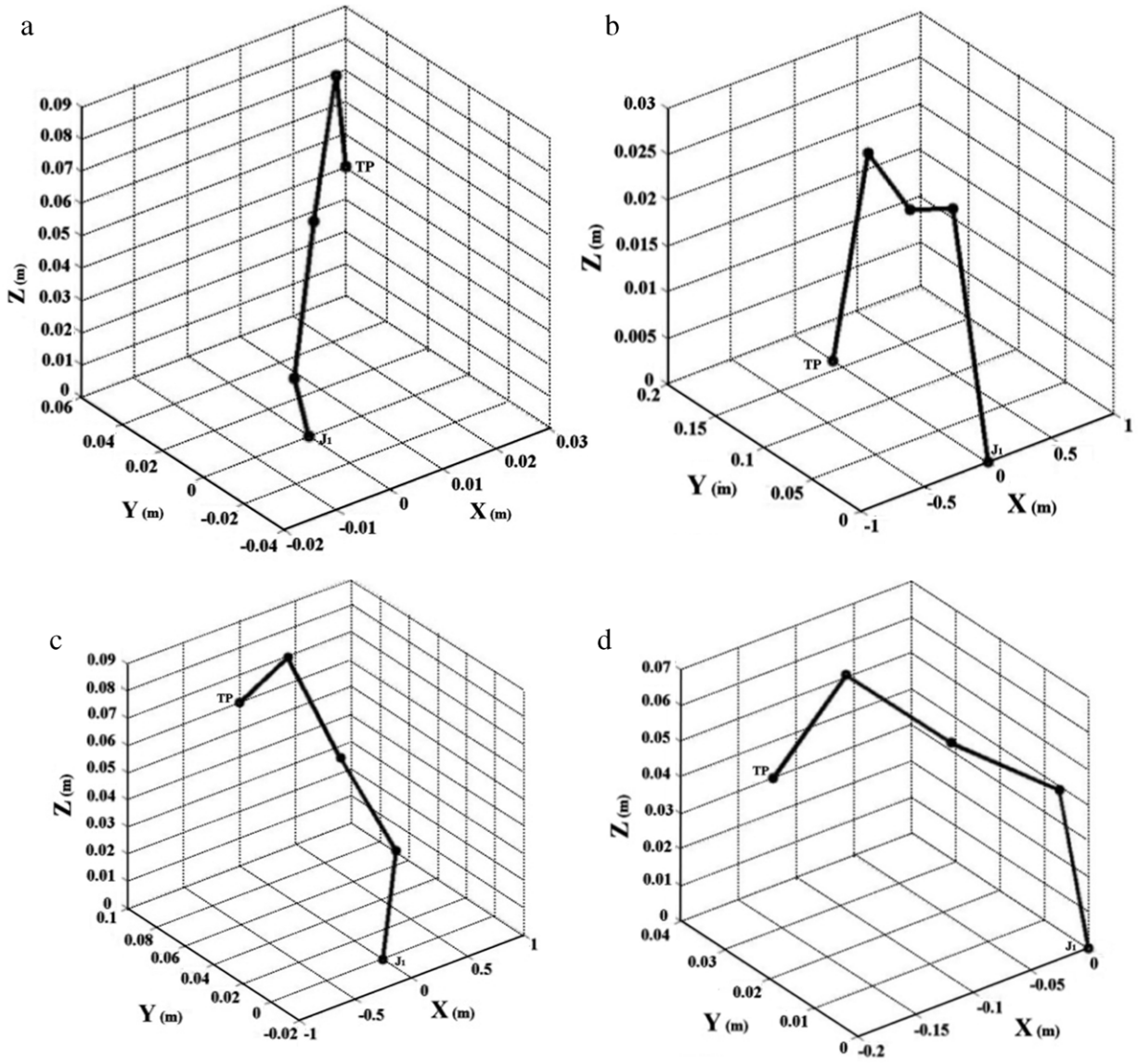

Fig. 10. Simulation results. (a) Plot for input target point (0.03, 0.06, 0.04). (b) Plot for input target point (0.0, 0.16, 0.0). (c) Plot for input target point (0.0, 0.1, 0.06). (d) Plot for input target point (−0.12, 0.04, 0.03).

with the irregularity. Fig. 9 shows the flowchart of the proposed method.

4. Simulation results

A simulation model has been developed in MATLAB for a 4 link redundant manipulator with $L_1 = L_2 = L_3 = L_4 = 0.044$ m. Some of the results obtained from this simulation are shown in Table 1.

The link configurations corresponding to data with serial number 1, 2, 3, 4 in Table 1 are shown in Fig. 10(a)–(d) respectively. From these figures one can see the workability of the proposed algorithm in finding out the inverse kinematic solution of the problem.

5. Experimental results

The approach developed in Section 2 has been tested on a 4 scaled model of the *In-Vivo* robot (as shown in Fig. 2). The length of each link is 0.044 m. The joint angles were obtained from the proposed method and the robot's joints were rotated to these angles with the help of wire actuation through servo motors. The final tip position of the robot was recorded for different cases and was compared with its corresponding input target point as shown in Fig. 11. For the simplicity of observation, the case of $Y = 0$ has been considered. Table 2 shows the numerical values of the

Table 2
Numerical values of the target point (simulation result), joint angles, and final tip positions (experimental results).

Sl. no.	Target point (m)	Joint angles (°)	Final tip position (m)
1	$X = 0.130,\ Y = 0,\ Z = 0.065$	$\theta_1 = 74.98, \theta_2 = 35.44, \theta_3 = 17.70, \theta_4 = -21.86, \phi = 90$	$X = 0.128, Y = 0, Z = 0.065$
2	$X = 0.080,\ Y = 0,\ Z = 0.145$	$\theta_1 = 88.89, \theta_2 = 65.45, \theta_3 = 56.77, \theta_4 = 33.33, \phi = 90$	$X = 0.080, Y = 0, Z = 0.146$
3	$X = 0,\ Y = 0,\ Z = 0.176$	$\theta_1 = 0, \theta_2 = 0, \theta_3 = 0, \theta_4 = 0, \phi = 90$	$X = 0, Y = 0, Z = 0.176$
4	$X = -0.080,\ Y = 0,\ Z = 0.145$	$\theta_1 = 146.67, \theta_2 = 123.23, \theta_3 = 114.55, \theta_4 = 91.11, \phi = 90$	$X = -0.086, Y = 0, Z = 0.144$

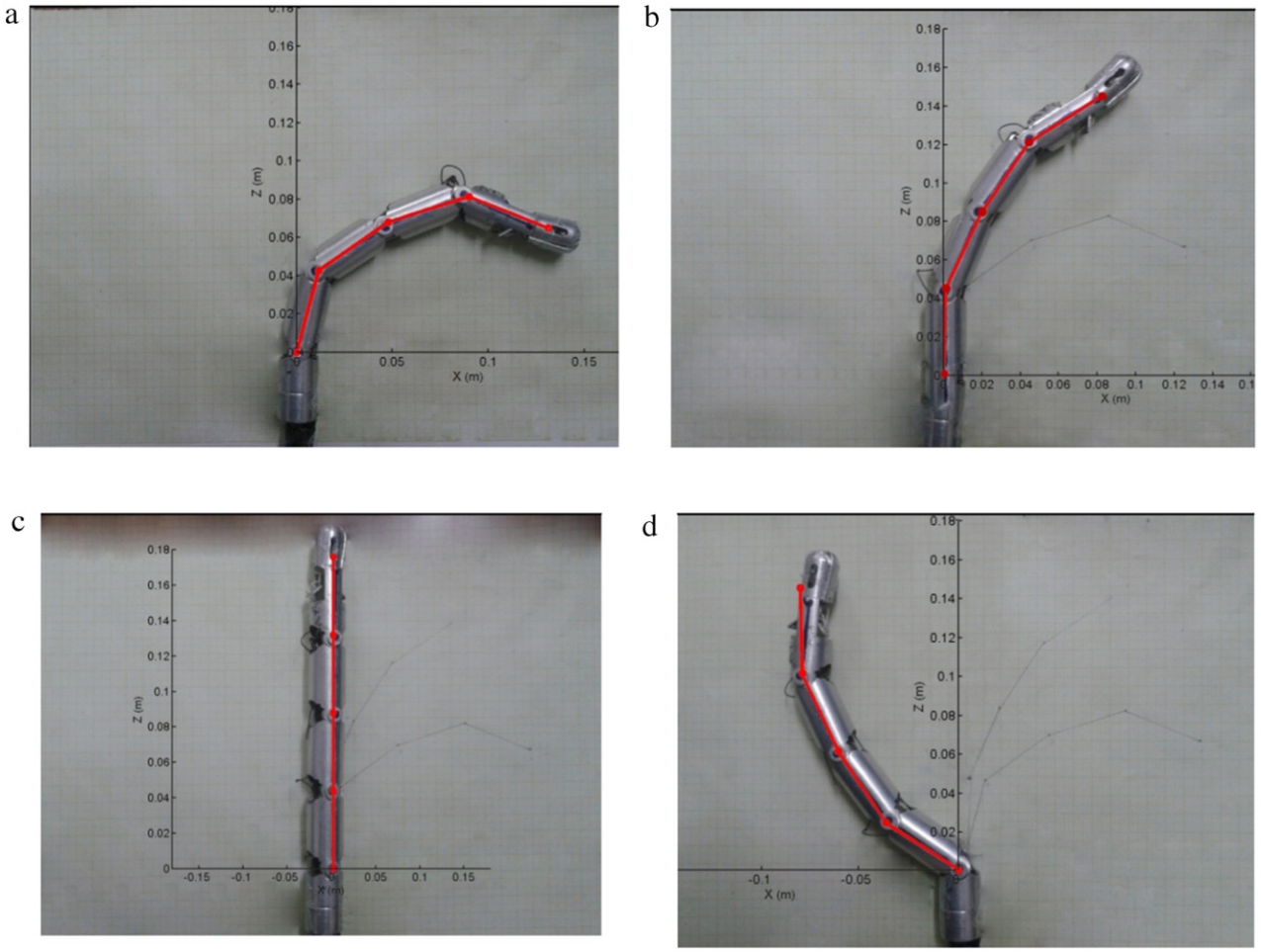

Fig. 11. Superimposed images of the actual positions of the robot and their corresponding simulation curves. TP (a) $X = 0.130, Y = 0, Z = 0.065$, (b) $X = 0.080, Y = 0, Z = 0.145$, (c) $X = 0.0, Y = 0, Z = 0.176$, (d) $X = 0.08, Y = 0, Z = 0.145$.

target point (simulation result), joint angles, and final tip positions (experimental results).

From Fig. 11 it is seen that for a given TP if the manipulator joints are rotated by the calculated angles (from the proposed inverse kinematics method), the final tip position is closely reached. The percentage of error for the target point and the final tip position are as given in Table 3. The percentages of errors were very low which further validates the proposed methodology.

6. Discussion

From Table 2 it is observed that the final tip positions obtained for different joint angles are close to the target points. The percentage of error indicated in Table 3 shows that in the 4th case there is a comparatively large error percentage of −7.5% of the final tip position with respect to the target point (TP) in the X direction.

The proposed methodology has been experimentally validated using the 4-scaled fabrication model of the *In-Vivo* robot. However for the actual size manipulator there are many challenges like the small diameter of the link of the manipulator and the hole through which the wire will be passed for wire actuation. The actual scale model size will be compatible with the surgical instrument i.e., it can be easily inserted through the available tool channel of the existing endoscope. The robot can have more links/joints. This will enable the robot to reach narrow cavities. Production of such a small size manipulator is possible through a rapid prototyping process using a laser sintering process. The wire actuation control unit along with the other controlling units, the base with the pulley and actuators will be stationed outside the abdominal cavity. The developed robot will be tested in a stomach like environment made of foam.

7. Conclusions

This paper presented an approach for inverse kinematics of a 4-link redundant manipulator for an *In-Vivo* robot for Biopsy using simple geometrical techniques. Future work can be done in this direction by extending this approach for the manipulators with an increased number of links and joints. In the present case, a twisted joint has been provided only at joint 1. Redundancy can

Table 3
Percentage of error of the final tip position with respect to the target point (TP).

Sl. no.	*X* direction (%)	*Y* direction (%)	*Z* direction (%)
1	1.538	0	0
2	0	0	−0.689
3	0	0	0
4	−7.5	0	0.689

be introduced in the *X*–*Y* plane also by providing twisting joints to other joints as well.

In real clinical situations, for particular surgical tasks there are much more parameters/factors needed to be considered in modelling, for example, the inserted force, inserted angle, trajectory and force applied on the deployed tool. Further experiments are to be carried out in order to develop an algorithm which will use the described approach to calculate the trajectory path and optimum configurations of the surgery robot on run-time using the input from different sensors. These experiments are proposed to be carried out using a 1X model of the *In-Vivo* robot.

The approach described in this paper is computationally fast and very simple in nature for solving inverse kinematics in the context of a surgical robot for biopsy. Through real experiments using a 4 scaled *In-Vivo* robot, it is shown that the proposed algorithm is accurate and provides flexibility in solving the joint angles of the robot.

Acknowledgement

We render our sincere gratitude to the Department of Science and Technology of Government of India for sponsoring this research (Scheme Grant Code SR/S3/MERC/048/2009).

References

[1] M.W. Hannan, I.D. Walker, Kinematics and the implementation of an elephant's trunk manipulator and other continuum style robots, Journal of Robotic Systems 20 (2) (2003) 45–63.
[2] J. Wang, Y. Li, X. Zhao, Inverse kinematics and control of a 7-DOF redundant manipulator based on the closed-loop algorithm, International Journal of Advanced Robotic Systems 7 (4) (2010) 1–9.
[3] E.S. Conkur, R. Buckingham, Clarifying the definition of redundancy as used in robotics, Robotica 15 (1997) 583–586. Cambridge University Press.
[4] P.J. McKerrow, Introduction to Robotics, Addison-Wesley Publishing Company, Sydney, 1991.
[5] X. Youshen, J. Wang, A dual neural network for kinematic control of redundant robot manipulators, IEEE Transactions on Systems, Man and Cybernetics 31 (1) (2001) 147–154.
[6] A.C. Nearchou, Solving the inverse kinematics problem of redundant robots operating in complex environments via a modified genetic algorithm, Mechanism and Machine Theory 33 (3) (1998) 273–292.
[7] A.R. Khoogar, J.K. Parker, Obstacle avoidance of redundant manipulators using genetic algorithms, in: IEEE Proceedings of Southeastcon'91, 07–10 April 1991, Williamsburg, VA, Vol. 1, 1991, pp. 317–320.
[8] A. Perez, J.M. McCarthy, Clifford algebra exponentials and planar linkage synthesis equations, Journal of Mechanical Design 127 (2005) 931–940.
[9] S. Yahya, M. Moghavvemi, H.A.F. Mohamed, Geometrical approach of planar hyper-redundant manipulators: inverse kinematics, path planning and workspace, Simulation Modelling Practice and Theory 19 (2011) 406–422.
[10] Z. Mao, T.C. Hsia, Obstacle avoidance inverse kinematics solution of redundant robots by neural networks, Robotica 15 (1) (1997) 3–10.
[11] I.A. Gravagne, I.D. Walker, Manipulability, force, and compliance analysis for planar continuum manipulators, Robotics and Automation 18 (3) (2002) 263–273.
[12] M.G. Marcos, J.A.T. Machado, T.P.A. Perdicoulis, An evolutionary approach for the motion planning of redundant and hyper-redundant manipulator, Nonlinear Dynamics 60 (2010) 115–119.
[13] J. Wang, Y. Li, X. Zhao, Inverse kinematics control of a 7-DOF redundant manipulator based on the closed-loop algorithm, Advanced Robotic Systems 7 (4) (2010) 1–10.
[14] J.W. Burdick, J. Radford, G.S. Chirikjian, A sidewinding locomotion gait for hyper-redundant robots, Advanced Robotics 9 (3) (1996) 195–216.
[15] G.S. Chirikjian, J.W. Burdick, Kinematically optimal hyper-redundant manipulator configurations, IEEE Transactions on Robotics and Automation 6 (11) (1995) 794–806.
[16] S. Neppali, M.A. Csencsits, B.A. Jones, I. Walker, A geometrical approach to inverse kinematics for continuum manipulator, in: IEEE/RSJ International Conference on Intelligent Robot and Systems, 22–26 September 2008, Nice France, 2008, pp. 3565–3570.
[17] I.E. Uphoff, G.S. Chirikjian, Inverse kinematics of discretely actuated hyper-redundant manipulators using workspace densities, in: Proceedings of the 1996 IEEE International Conference on Robotics and Automation, 22–28 April 1996, Minneapolis, Minnesota, Vol. 1, 1996, pp. 139–145.
[18] G.S. Chirikjian, J.W. Burdick, Parallel formulation of the inverse kinematics of modular hyper-redundant manipulators, in: IEEE International Conference on Robotics and Automation, Sacramento, 9–11 April 1991, California, Vol. 1, 1991, pp. 708–713.
[19] G.S. Chirikjian, A general numerical method for hyper-redundant manipulator inverse kinematics, in: Proceedings of IEEE International Conference on Robotics and Automation, 2–6 May 1993, Atlanta, GA, Vol. 3, 1993, pp. 107–111.
[20] B. Jones, I.D. Walker, Kinematics for multi-section continuum robots, IEEE Transactions on Robotics 22 (1) (2006) 43–55.
[21] S. Sreenivasan, P. Goel, A. Ghosal, A real-time algorithm for simulation of flexible objects and hyper-redundant manipulators, Mechanism and Machine Theory 45 (2010) 454–466.
[22] M.K. Sutar, P.M. Pathak, A.K. Sharma, N.K. Mehta, V.K. Gupta, Forward kinematic analysis of in-vivo robot for stomach biopsy, Journal of Robotic Surgery (2012). http://dx.doi.org/10.1007/s11701-012-0375-y.

Lokesh Sardana is a B.Tech. student in the Department of Mechanical and Industrial Engineering Department, Indian Institute of Technology Roorkee, Roorkee. His areas of interest are robotics and mechatronics.

Mihir Kumar Sutar is a Research Scholar at the Robotics and Control Laboratory, Department of Mechanical and Industrial Engineering, Indian Institute of Technology Roorkee, Roorkee and is currently pursuing his Ph.D. His area of research is Dynamics and Control of In-Vivo Robots.

Pushparaj Mani Pathak has been an Associate Professor at the Mechanical and Industrial Engineering Department, Indian Institute of Technology Roorkee, Roorkee since 2006. He obtained the B.Tech. from NIT Calicut, the M.Tech. in Solid Mechanics and Design from IIT Kanpur and the Ph.D. in the area of Space Robotics from the Indian Institute of Technology Kharagpur, Kharagpur. His research interests are space robotics, walking robots, In-Vivo robot dynamics and control.